

# An augmented Lagrangian deep learning method for variational problems with essential boundary conditions

Jianguo Huang (jghuang@sjtu.edu.cn)

School of Mathematical Sciences, and MOE-LSC, Shanghai Jiao Tong University, Shanghai, China

Haoqin Wang (wanghaoqin@sjtu.edu.cn)

School of Mathematical Sciences, and MOE-LSC, Shanghai Jiao Tong University, Shanghai, China

Tao Zhou\*(tzhou@lsec.cc.ac.cn)

LSEC, Institute of Computational Mathematics and Scientific/Engineering Computing,  
Academy of Mathematics and Systems Science, Chinese Academy of Sciences, Beijing, China

## Abstract

This paper is concerned with a novel deep learning method for variational problems with essential boundary conditions. To this end, we first reformulate the original problem into a minimax problem corresponding to a feasible augmented Lagrangian, which can be solved by the augmented Lagrangian method in an infinite dimensional setting. Based on this, by expressing the primal and dual variables with two individual deep neural network functions, we present an augmented Lagrangian deep learning method for which the parameters are trained by the stochastic optimization method together with a projection technique. Compared to the traditional penalty method, the new method admits two main advantages: i) the choice of the penalty parameter is flexible and robust, and ii) the numerical solution is more accurate in the same magnitude of computational cost. As typical applications, we apply the new approach to solve elliptic problems and (nonlinear) eigenvalue problems with essential boundary conditions, and numerical experiments are presented to show the effectiveness of the new method.

**Keywords.** The augmented Lagrangian method; Deep learning; Variational problems; Saddle point problems; Essential Boundary Conditions.

**AMS subject classifications:** 65N99, 68T05.

## 1 Introduction

Variational problems play important roles in various industrial and engineering applications, with typical examples including partial differential equations (PDEs) and eigenvalue problems. Many classical numerical methods have been developed for such problems, e.g., the finite difference method, the spectral method, and the finite element method. The first two methods are generally used for solving problems over regular domains while the latter one is particularly suitable for problems in irregular domains [6, 11]. In recent years, deep learning based techniques have been widely used to solve a variety of variational problems [9, 14, 16, 18, 22, 23, 27, 30, 33, 35, 36].

---

\*Corresponding author

Historically, related studies can date back to the 1990s [12, 25]. We also refer the reader to [13] and the references therein for a comprehensive review on machine learning from the perspective of computational mathematics. For such kind of methods, deep neural networks (DNNs) are exploited to parameterize the PDE solutions and appropriate parameters are identified by minimizing an optimization problem formulated from the PDEs. The most significant feature of those methods is that they are mesh-free, and their approximation capacity has been well studied in recent years [3, 15, 19, 21, 31].

For variational problems with natural boundary conditions, one doesn't need to impose these conditions on the admissible functions [16], so that the DNNs can easily be used for approximation. However, for variational problems with essential boundary conditions, these conditions should be imposed on the admissible functions, and this gives rise to a significant difficulty since one cannot enforce the boundary condition in a simple way even at the interpolation nodes for a neural network function. It is worth noting that even in the context of finite element methods, this is also a very tough issue. In fact, one has to use Nitsche's trick [28], developed further by Stenberg [34], to handle this issue. As far as we know, there are two main strategies to overcome the bottleneck in deep learning framework:

- The first strategy is to construct neural network functions that satisfy the essential boundary conditions exactly. For instance, if the boundary condition is given by  $u = g$  on the boundary  $\Gamma$ , then we construct the approximate function by

$$\phi(\mathbf{x}; \boldsymbol{\theta}) = \ell(\mathbf{x})\psi(\mathbf{x}; \boldsymbol{\theta}) + \bar{g}(\mathbf{x}), \quad (1.1)$$

where  $\ell(\mathbf{x})$  is a known function such that on  $\Gamma$  it holds  $\ell(\mathbf{x}) = 0$ ,  $\bar{g}$  is the extension of  $g$  to the whole domain, and  $\psi(\mathbf{x}; \boldsymbol{\theta})$  is another neural network function that is used to approximate the solution in the domain. The main limitation of this approach is that for problems with complex (non-regular) domain, it is in general not easy to find explicit functions  $\ell$  and  $\bar{g}$ . For details, one can refer to [4] and references therein. It is worth mentioning that based on the formulation (1.1), one can also introduce an additional neural network function on the boundary  $\Gamma$  to approximate  $g$  by a least squares approach [32].

- Another strategy is the penalty method, where a penalty term (with a penalty parameter  $\beta$ ) is included into the objective functional to enforce the boundary condition [16, 30, 33, 35]. This method is easy to implement. Theoretically, the penalty parameter  $\beta$  should be chosen large enough, however, this may make the optimization problem become ill-conditioned [29]. We also mention the deep Nitsche method proposed in [26], where Nitsche's variational formula is used for the second order elliptic problems to avoid a large penalty parameter.

In this work, we intend to present an augmented Lagrangian deep learning (ALDL) method to handle variational problems with essential boundary conditions. For this purpose, we shall first rewrite the original problem as a minimax problem associated with a feasible augmented Lagrangian, which can be solved by the augmented Lagrangian method in an infinite dimensional setting [17, 29]. We then express the primal and dual variables with two individual DNN functions, respectively, and train the associated network parameters with the stochastic optimization method (based on the augmented Lagrangian method). It is worth noting that we require to solve a least square problem in order to update the dual variable, and this step can be viewed as a nonlinear projection in the corresponding parameter space. As typical applications, we apply the ALDL method to solve elliptic problems and eigenvalue problems with essential boundary conditions. Numerical results indicate that the ALDL method admits two main advantages compared to the penalty method:

- The choice of the penalty parameter is flexible and robust.
- The numerical solution is more accurate in the same magnitude of computational cost.

The rest of this paper is organized as follows. In Section 2, we introduce the variational problem and its minimax formulation. As typical cases, an elliptic PDE and eigenvalue problems are presented. In Section 3, we recall the augmented Lagrangian method in an infinite dimensional setting, and then propose the augmented Lagrangian deep learning method. In Section 4, numerical examples are reported to show the performance of the proposed method. Finally, we provide with some concluding remarks in Section 5.

## 2 The variational problem and its primal-dual formulation

To begin, we first introduce some notations for later uses. For a real Hilbert space  $V$  equipped with a norm  $\|\cdot\|_V$ , we denote by  $\langle \cdot, \cdot \rangle_V$  the induced inner product over  $V$ . We use the standard symbols and notations for Sobolev space and their norms or semi-norms and refer the reader to the reference [1] for details. Let  $\Omega \subset \mathbb{R}^d$  be a bounded domain with Lipschitz boundary, where  $d$  is a natural number. We also denote by  $\Gamma$  its boundary and  $\bar{\Omega}$  the closure of  $\Omega$ , respectively. We let  $B$  be a bounded linear operator from  $V$  to another Hilbert space  $W$  and a typical example in our variational problems is  $W = L^2(\Gamma)$ .

Throughout this paper, we consider the following variational problem

$$\min_{v \in V_g} J(v), \quad (2.1)$$

where  $J(v)$  is a nonlinear functional over  $V_g$  and

$$V_g = \{v \in V : Bv = g \text{ on } \Gamma\}.$$

### 2.1 Primal-dual formulation

To deal with the constraint in the admissible set  $V_g$ , the augmented Lagrangian method [17] suggests to consider an augmented Lagrangian function as following

$$\mathcal{L}_\beta(v, \mu) = J(v) - \langle \mu, Bv - g \rangle_W + \frac{\beta}{2} \|Bv - g\|_W^2, \quad (2.2)$$

where  $\mu \in W$  is a Lagrange multiplier function (the dual variable) and  $\beta$  is a positive constant. Then we obtain the following minimax problem:

$$\min_{v \in V} \max_{\mu \in W} \mathcal{L}_\beta(v, \mu). \quad (2.3)$$

By a direct manipulation, we have

$$\max_{\mu \in W} \mathcal{L}_\beta(v, \mu) = \begin{cases} J(v), & v \in V_g, \\ +\infty, & v \notin V_g. \end{cases}$$

Consequently, the variational problem (2.1) is equivalent to the minimax problem (2.3). In other words, if  $(u, \lambda) \in V \times W$  is a solution of the problem (2.3), then  $u$  is a solution of the problem (2.1). On the contrary, if  $u$  is a solution of the problem (2.1), there exists a function  $\lambda \in W$  such

that  $(u, \lambda)$  is a solution of the problem (2.3). Furthermore, we assume that  $(u, \lambda)$  is a saddle point of the Lagrangian  $\mathcal{L}_\beta(\cdot, \cdot)$ , i.e.,

$$\min_{v \in V} \max_{\mu \in W} \mathcal{L}_\beta(v, \mu) = \mathcal{L}_\beta(u, \lambda) = \max_{\mu \in W} \min_{v \in V} \mathcal{L}_\beta(v, \mu). \quad (2.4)$$

Notice that it is rather difficult to show the existence of a saddle point of a general functional and one important technique is the Ky Fan-Sion theorem [8]. If we write

$$\mathcal{F}_\beta(\mu) = \min_{v \in V} \mathcal{L}_\beta(v, \mu),$$

then one can turn to solve the following dual problem

$$\max_{\mu \in W} \mathcal{F}_\beta(\mu). \quad (2.5)$$

## 2.2 Some applications

We now present three typical applications of the above primal dual formulation.

### 2.2.1 Second order elliptic PDEs

The first example is the second order elliptic equations:

$$\begin{cases} -\operatorname{div}(\mathbf{A}(\mathbf{x})\nabla u(\mathbf{x})) + c(\mathbf{x})u(\mathbf{x}) = f(\mathbf{x}) & \text{in } \Omega, \\ u(\mathbf{x}) = g(\mathbf{x}), & \text{on } \Gamma, \end{cases} \quad (2.6)$$

where  $\mathbf{A}(\mathbf{x}) \in C^1(\bar{\Omega})$  is uniformly elliptic and  $c(\mathbf{x}) \in L^2(\Omega)$  is nonnegative over  $\Omega$ .

The variational formula of (2.6) is

$$\min_{v \in V_g} J(v), \quad (2.7)$$

where

$$J(v) = \frac{1}{2} \int_{\Omega} [\mathbf{A}(\mathbf{x})\nabla v(\mathbf{x}) \cdot \nabla v(\mathbf{x}) + c(\mathbf{x})v^2(\mathbf{x}) - 2f(\mathbf{x})v(\mathbf{x})] \, dx,$$

and

$$V_g = \{v \in H^1(\Omega) : v = g \text{ a.e. on } \Gamma\}.$$

Based on the abstract setting given in the last subsection, we can rewrite the variational formula (2.7) as the following problem

$$\min_{v \in V} \max_{\mu \in W} \mathcal{L}_\beta(v, \mu), \quad \mathcal{L}_\beta(v, \mu) = J(v) - \int_{\Gamma} [\mu(\mathbf{x})(v(\mathbf{x}) - g(\mathbf{x}))] \, dx + \frac{\beta}{2} \int_{\Gamma} [v(\mathbf{x}) - g(\mathbf{x})]^2 \, dx, \quad (2.8)$$

where  $V = H^1(\Omega)$ ,  $W = L^2(\Gamma)$ , and  $\beta$  is a positive parameter. As shown in [10], there exists a unique saddle point for the above problem.

### 2.2.2 Linear eigenvalue problems

The second example is the eigenvalue problems. Suppose we want to find the smallest eigenvalue and its eigenfunction for a positive self-adjoint differential operator, e.g.,

$$\begin{cases} -\nabla \cdot (p(\mathbf{x}) \nabla u(\mathbf{x})) + q(\mathbf{x})u(\mathbf{x}) = \rho u(\mathbf{x}) & \text{in } \Omega, \\ u(\mathbf{x}) = 0 & \text{on } \Gamma, \end{cases} \quad (2.9)$$

where  $p(\mathbf{x}) \in C^1(\bar{\Omega})$  is uniformly elliptic and  $q(\mathbf{x}) \in C(\bar{\Omega})$  is nonnegative over  $\Omega$ .

The variational formula of 2.9 (cf. [2]) is

$$\min_{v \in V_0} J(v), \quad J(v) = \frac{\int_{\Omega} [p(\mathbf{x}) \nabla v(\mathbf{x}) \cdot \nabla v(\mathbf{x}) + q(\mathbf{x})v^2(\mathbf{x})] dx}{\int_{\Omega} v^2(\mathbf{x}) dx}, \quad (2.10)$$

where  $V_0 = H_0^1(\Omega)$ .

Suppose  $(\rho, u)$  is the solution of (2.9). Then it is easy to check  $(\rho, cu)$  is also a solution of (2.9), where  $c$  is a non-zero real number. This motivates us to find the normalized eigenfunction, i.e.,

$$\min_{v \in V_0} \tilde{J}(v), \quad \tilde{J}(v) = \int_{\Omega} [p(\mathbf{x}) \nabla \tilde{v}(\mathbf{x}) \cdot \nabla \tilde{v}(\mathbf{x}) + q(\mathbf{x})\tilde{v}^2(\mathbf{x})] dx, \quad (2.11)$$

where  $\tilde{v} = v/\|v\|_{0,\Omega}$ . As mentioned above, we can reformulate (2.11) as the following minimax problem

$$\min_{v \in V} \max_{\mu \in W} \mathcal{L}_{\beta}(v, \mu), \quad \mathcal{L}_{\beta}(v, \mu) = \tilde{J}(v) - \int_{\Gamma} \mu(\mathbf{x}) \tilde{v}(\mathbf{x}) dx + \frac{\beta}{2} \int_{\Gamma} \tilde{v}^2(\mathbf{x}) dx, \quad (2.12)$$

where  $V = H^1(\Omega)$ ,  $W = L^2(\Gamma)$  and  $\beta$  is a positive parameter.

### 2.2.3 Nonlinear eigenvalue problems

The third example is a nonlinear eigenvalue problem:

$$\begin{cases} -\nabla \cdot (\mathbf{A}(\mathbf{x}) \nabla u(\mathbf{x})) + V(\mathbf{x})u(\mathbf{x}) + u^3(\mathbf{x}) = \rho u(\mathbf{x}) & \text{in } \Omega, \\ u(\mathbf{x}) = 0 & \text{on } \partial\Omega, \\ \|u\|_{0,\Omega} = 1, \end{cases} \quad (2.13)$$

where  $\mathbf{A}(\mathbf{x}) \in (L^\infty(\Omega))^{d \times d}$  is symmetric and uniformly elliptic, and  $V(\mathbf{x}) \in L^2(\Omega)$ .

The variational formula of (2.13) (cf. [7]) is

$$\min_{\substack{v \in V_0 \\ \|v\|_{0,\Omega}=1}} J(v), \quad J(v) = \frac{1}{2} \int_{\Omega} [\mathbf{A}(\mathbf{x}) \nabla v(\mathbf{x}) \cdot \nabla v(\mathbf{x}) + V(\mathbf{x})v^2(\mathbf{x}) + v^4(\mathbf{x})] dx, \quad (2.14)$$

where  $V_0 = H_0^1(\Omega)$ . According to reference [7], the ground state non-negative solution  $(\rho, u)$  of (2.14) is unique for  $1 \leq d \leq 3$ . Similar to linear eigenvalue problems, we use the normalization technique to relax the constraint  $\|v\|_{0,\Omega} = 1$ , and then reformulate the variational problem (2.14) as

$$\min_{v \in V_0} \tilde{J}(v), \quad \tilde{J}(v) = \frac{1}{2} \int_{\Omega} [\mathbf{A}(\mathbf{x}) \nabla \tilde{v}(\mathbf{x}) \cdot \nabla \tilde{v}(\mathbf{x}) + V(\mathbf{x})\tilde{v}^2(\mathbf{x}) + \tilde{v}^4(\mathbf{x})] dx, \quad (2.15)$$

where  $\tilde{v} = v/\|v\|_{0,\Omega}$ . As discussed in Section 2.1, we can rewrite the variational formula (2.15) as the minimax problem

$$\min_{v \in V} \max_{\mu \in W} \mathcal{L}_{\beta}(v, \mu), \quad \mathcal{L}_{\beta}(v, \mu) = \tilde{J}(v) - \int_{\Gamma} \mu(\mathbf{x}) \tilde{v}(\mathbf{x}) dx + \frac{\beta}{2} \int_{\Gamma} \tilde{v}^2(\mathbf{x}) dx, \quad (2.16)$$

where  $V = H^1(\Omega)$ ,  $W = L^2(\Gamma)$  and  $\beta$  is a positive parameter.

### 3 An augmented Lagrangian deep learning method

Before presenting our augmented Lagrangian deep learning method, we first recall the augmented Lagrangian method for the minimax problem (2.3) in a Hilbert space setting [17].

The main idea here is to find the saddle point by solving the dual problem (2.5). More precisely, one may first fix the primal variable  $v_k$  at the  $k$ th iteration, and update the dual variable to  $\mu_{k+1}$ . Then we fix the approximate dual variable  $\mu_{k+1}$  and find an approximate minimizer  $v_{k+1}$ . The method is summarized in Algorithm 1.

---

**Algorithm 1** The augmented Lagrangian method.

---

**Input:** The parameter  $\beta_0 > 0$ , tolerance  $\tau_0 > 0$ , increase parameter  $\alpha \geq 1$ , initial guess  $v_0, \mu_0$ , max iteration number  $Epoch$ .

**for**  $k = 0, 1, \dots, Epoch$  **do**

    Update Lagrange multiplier function  $\mu$  by

$$\mu_k = \mu_{k-1} - \beta_k(Bv_k - g) \quad (\star)$$

**while**  $\|\partial_1 \mathcal{L}_\beta(v_k, \mu_k)\| > \tau_k$  **do**

        Fix  $\mu_k$  and find a minimizer  $v_k$  of  $\mathcal{L}_\beta(v, \mu_k)$ .

**end while**

    Set  $v_{k+1} = v_k$ .

    Update penalty parameter by  $\beta_{k+1} = \alpha\beta_k$ .

    Select new tolerance  $\tau_{k+1}$ .

**end for**

**Output:**  $u = v_{Epoch}, \lambda = \mu_{Epoch}$ .

---

We now present some basic concepts of the deep neural networks (DNNs). In this paper, we shall adopt the residual neural network (ResNet) proposed in [20] to approximate the variational problem. The ResNet can be formulated as follow:

$$\mathbf{h}_0 = \mathbf{V}\mathbf{x}, \mathbf{h}_\ell = \mathbf{h}_{\ell-1} + \sigma(\mathbf{W}_\ell \mathbf{h}_{\ell-1} + \mathbf{b}_\ell), \ell = 1, 2, \dots, L, \phi(\mathbf{x}; \boldsymbol{\theta}) = \mathbf{a}^T \mathbf{h}_L,$$

where  $\mathbf{V} \in \mathbb{R}^{N \times d}$ ,  $\mathbf{W}_\ell \in \mathbb{R}^{N \times N}$ ,  $\mathbf{b}_\ell \in \mathbb{R}^N$  for  $\ell = 1, \dots, L$ ,  $\mathbf{a} \in \mathbb{R}^N$ .  $\sigma(x)$  is a non-linear activation function. Here,  $L$  is the depth of the ResNet, and  $N$  is the width of the network.  $\boldsymbol{\theta} = \{\mathbf{V}, \mathbf{a}, \mathbf{W}_\ell, \mathbf{b}_\ell : 1 \leq \ell \leq L\}$  denotes the set of all parameters in  $\phi$ , which uniquely determines the neural network.

To present the augmented Lagrangian deep learning method, we express the primal and dual variables with two individual DNN functions, respectively, i.e.,

$$u(\mathbf{x}) \approx \phi^u(\mathbf{x}; \boldsymbol{\theta}_u), \quad \lambda(\mathbf{x}) \approx \phi^\lambda(\mathbf{x}; \boldsymbol{\theta}_\lambda).$$

To derive the numerical solution, it suffices for us to determine parameters  $\boldsymbol{\theta}_u$  and  $\boldsymbol{\theta}_\lambda$ . To this end, we may closely follow the strategies given in Algorithm 1. Notice that one can directly follow Algorithm 1 to update the primal variable, however, for the dual variable, Algorithm 1 is not directly applicable since we need to update the parameters of the neural networks (not a function itself). In other words, we cannot directly update the parameters  $\boldsymbol{\theta}_\mu$  of the dual variable  $\phi^\mu$  through the equation  $(\star)$ , i.e.,

$$\phi_{k+1}^\mu \Leftarrow \phi_k^\mu - \beta_k(B\phi_k^v - g).$$

To overcome this difficulty, we propose to solve the following least squares problem:

$$\phi_{k+1}^\mu = \arg \min_{\boldsymbol{\theta}_\nu} J_\lambda(\phi^\nu; \phi_k^\mu, \phi_k^v), \quad J_\lambda(\phi^\nu; \phi_k^\mu, \phi_k^v) = \|\phi^\nu(\mathbf{x}; \boldsymbol{\theta}_\nu) - \phi_k^\mu(\mathbf{x}; \boldsymbol{\theta}_\mu) - \beta_k(B\phi_k^v(\mathbf{x}; \boldsymbol{\theta}_v) - g(\mathbf{x}))\|_L^2. \quad (3.1)$$

Notice that the functionals  $\mathcal{L}_\beta(v, \mu)$  and  $J_\lambda(\nu; \mu_k, v)$  can be expressed as integrals over  $\Omega$  or  $\Gamma$  in most cases, meaning that sub-optimization problems involved can be solved by means of the stochastic gradient descent method [5, 24].

To sum up the above discussions, we summarize our augmented Lagrangian deep learning method in Algorithm 2.

---

**Algorithm 2** The augmented Lagrangian deep learning method.

---

**Input:** The parameter  $\beta_0 > 0$ , tolerance  $\tau_0 > 0$ , increase parameter  $\alpha \geq 1$ , the iteration number  $Epoch$ , the iteration number of model  $Epoch_u$ , the iteration number of Lagrange multiplier  $Epoch_\lambda$ .

Initialize the approximation  $\phi_0^v(\mathbf{x}; \boldsymbol{\theta}_v)$  and  $\phi_0^\mu(\mathbf{x}; \boldsymbol{\theta}_\mu)$  following the default random initialization of PyTorch.

**for**  $k = 0, 1, \dots, Epoch$  **do**

**for**  $l = 0, 1, \dots, Epoch_\lambda$  **do**

        Fix the parameter  $\boldsymbol{\theta}_v$  of  $\phi_k^v$  and optimize the problem

$$\min_{\boldsymbol{\theta}_v} J_\lambda(\phi^v(\mathbf{x}; \boldsymbol{\theta}_v); \phi_k^\mu, \phi_k^v).$$

**end for**

    Set  $\phi_{k+1}^\mu = \phi^v(\mathbf{x}; \boldsymbol{\theta}_\mu)$ .

**for**  $l = 0, 1, \dots, Epoch_u$  **do**

        Fix the parameter  $\boldsymbol{\theta}_\mu$  of  $\phi_{k+1}^\mu$  and optimize the problem

$$\min_{\boldsymbol{\theta}_v} \mathcal{L}_\beta(\phi^v(\mathbf{x}; \boldsymbol{\theta}_v), \phi_{k+1}^\mu).$$

**end for**

    Set  $\phi_{k+1}^v = \phi^v(\mathbf{x}; \boldsymbol{\theta}_v)$ .

    Update penalty parameter by  $\beta_{k+1} = \alpha\beta_k$ .

**end for**

**Output:**  $u = \phi_{Epoch+1}^v$ ,  $\lambda = \phi_{Epoch+1}^\mu$ .

---

Next, we present some details for implementing the ALDL method. For the elliptic problems 2.6, we have

$$\begin{aligned} \mathcal{L}_\beta(v, \mu) &= \frac{1}{2} \int_{\Omega} [\mathbf{A}(\mathbf{x}) \nabla v(\mathbf{x}) \cdot \nabla v(\mathbf{x}) + c(\mathbf{x}) v^2(\mathbf{x}) - 2f(\mathbf{x}) v(\mathbf{x})] dx \\ &\quad - \int_{\Gamma} [\mu(\mathbf{x})(v(\mathbf{x}) - g(\mathbf{x}))] dx + \frac{\beta}{2} \int_{\Gamma} [v(\mathbf{x}) - g(\mathbf{x})]^2 dx \\ &= |\Omega| \mathbb{E}_{\boldsymbol{\xi}} \left[ \frac{1}{2} \mathbf{A}(\boldsymbol{\xi}) |\nabla v(\boldsymbol{\xi})|^2 + \frac{1}{2} c(\boldsymbol{\xi}) v^2(\boldsymbol{\xi}) - f(\boldsymbol{\xi}) v(\boldsymbol{\xi}) \right] \\ &\quad - |\Gamma| \mathbb{E}_{\boldsymbol{\eta}} \left[ \mu(\boldsymbol{\eta})(v(\boldsymbol{\eta}) - g(\boldsymbol{\eta})) + \frac{\beta}{2} (v(\boldsymbol{\eta}) - g(\boldsymbol{\eta}))^2 \right], \end{aligned} \quad (3.2)$$

where  $\boldsymbol{\xi}$  and  $\boldsymbol{\eta}$  are random vectors following the uniform distribution over  $\Omega$  and  $\Gamma$ , respectively.  $|\Omega|$  and  $|\Gamma|$  is the measure of  $\Omega$  and  $\Gamma$ , respectively.

By the definition of  $J_\lambda(\nu; v)$ , we have

$$J_\lambda(\nu; \mu_k, v) = \int_{\Gamma} [\nu(\mathbf{x}) - \mu_k(\mathbf{x}) - \beta(v(\mathbf{x}) - g(\mathbf{x}))]^2 dx = |\Gamma| \mathbb{E}_{\boldsymbol{\eta}} \left[ (\nu(\boldsymbol{\eta}) - \mu_k(\boldsymbol{\eta}) - \beta(v(\boldsymbol{\eta}) - g(\boldsymbol{\eta})))^2 \right]. \quad (3.3)$$

Upon substituting (3.2) and (3.3) into Algorithm 2, one can then obtain the ALDL algorithm.

As for the linear eigenvalue problem, a direct manipulation gives

$$\mathcal{L}_\beta(v, \mu) = \frac{\mathbb{E}_\xi[p(\xi)|\nabla v(\xi)|^2 + q(\xi)v^2(\xi)]}{\mathbb{E}_\zeta[v^2(\zeta)]} - \frac{|\Gamma|\mathbb{E}_\eta[\mu(\eta)v(\eta)]}{\sqrt{|\Omega|\mathbb{E}_\zeta[v^2(\zeta)]}} + \frac{\beta|\Gamma|\mathbb{E}_\eta[v^2(\eta)]}{2|\Omega|\mathbb{E}_\zeta[v^2(\zeta)]}, \quad (3.4)$$

$$J_\lambda(\nu; \mu_k, \tilde{v}_k) = |\Gamma|\mathbb{E}_\eta \left[ (\nu(\eta) - \mu_k(\eta) - \beta\tilde{v}_k(\eta))^2 \right] = |\Gamma|\mathbb{E}_\eta \left[ \left( \nu(\eta) - \mu_k(\eta) - \beta \frac{v_k(\eta)}{\|v_k\|_{0,\Omega}} \right)^2 \right], \quad (3.5)$$

where  $\xi, \zeta$  are i.i.d. random vectors following the uniform distribution over  $\Omega$ , and  $\eta$  is the random vector following the uniform distribution over  $\Gamma$ . Notice that  $\tilde{v}_k$  is fixed in  $J_\lambda(\nu; \mu_k, \tilde{v}_k)$ , so  $\|v_k\|_{0,\Omega}$  is a known real number in  $J_\lambda(\nu; \mu_k, \tilde{v}_k)$ . Again, one may obtain the DLAL algorithm for eigenvalue problems by substituting the above formulas into Algorithm 2.

For the nonlinear eigenvalue problem (2.13), we have

$$\begin{aligned} \mathcal{L}_\beta(v, \mu) &= \frac{\mathbb{E}_{\xi_1}[A(\xi_1)|\nabla v(\xi_1)|^2 + V(\xi_1)v^2(\xi_1)]}{\mathbb{E}_{\xi_2}[v^2(\xi_2)]} + \frac{\mathbb{E}_{\xi_1}[v^4(\xi_1)]}{|\Omega|\mathbb{E}_{\xi_2, \xi_3}[v^2(\xi_2)v^2(\xi_3)]} \\ &\quad - \frac{|\Gamma|\mathbb{E}_\eta[\mu(\eta)v(\eta)]}{\sqrt{|\Omega|\mathbb{E}_{\xi_2}[v^2(\xi_2)]}} + \frac{\beta|\Gamma|\mathbb{E}_\eta[v^2(\eta)]}{2|\Omega|\mathbb{E}_{\xi_2}[v^2(\xi_2)]}, \end{aligned} \quad (3.6)$$

$$J_\lambda(\nu; \mu_k, \tilde{v}_k) = |\Gamma|\mathbb{E}_\eta \left[ (\nu(\eta) - \mu_k(\eta) - \beta\tilde{v}_k(\eta))^2 \right] = |\Gamma|\mathbb{E}_\eta \left[ \left( \nu(\eta) - \mu_k(\eta) - \beta \frac{v_k(\eta)}{\|v_k\|_{0,\Omega}} \right)^2 \right], \quad (3.7)$$

where  $\xi_1, \xi_2, \xi_3$  are i.i.d. random vectors produced by the uniform distribution over  $\Omega$ , and  $\eta$  is the random vectors following the uniform distribution over  $\Gamma$ .

## 4 Numerical experiments

In this section, we shall present various numerical examples to illustrate the effectiveness of the ALDL method. We shall also perform a numerical comparison between the penalty method (PMDL) and the ALDL method. In all our numerical examples, we shall use the ResNet with width  $N = 50$  and depth  $L = 6$  with an activation function  $\sigma(x) = \max\{x^2, 0\}$  to approximate the solution  $u$ , which results in 15350 unknown parameters. To reduce the computation cost, we use a ResNet with width  $N = 50$  and depth  $L = 2$  with an activation function  $\sigma(x) = \max\{x^2, 0\}$  as an approximation to the dual variable  $\lambda$ , which results in 5150 parameters.

We use the Adam optimizer [24] for training, with a learning rate  $\eta = 1e - 3$  for elliptic PDEs, and  $\eta = 5e - 4$  for eigenvalue problems. The maximum iteration number  $Epoch$  is taken as 50000 for the PMDL method, and we set  $Epoch = 500$ ,  $Epoch_\lambda = 100$  and  $Epoch_u = 100$  for the ALDL method. The batch size within the computation domain is 512. While the number of training points on the [each](#) boundary is set to be 64 for all problems. All numerical experiments are implemented in Python 3.7 using Pytorch 1.3 in an NVIDIA GEFORCE RTX 2080 Ti GPU card.

For elliptic PDEs, we use  $u$  and  $u_{dl}$  to denote the exact solution and the deep learning solution, respectively. While for eigenvalue problems, we let  $\rho$  and  $u$  be the smallest eigenvalue and the corresponding eigenfunction with  $\|u\|_0 = 1$ , respectively. Also, we denote by  $\rho_{dl}$  and  $u_{dl}$  the DNNs solutions. For a computational domain  $\Omega = (0, 1)^d$ , we divide it into small cubes with a length  $h$  uniformly and denote the set of all vertexes as  $\Omega_h$ , i.e.,  $\Omega_h = \{ih : 0 \leq i \leq N\}^d$  with  $N = 1/h$ . We shall test the numerical accuracy on  $\Omega_h$ . In order to measure the accuracy of deep learning



algorithms, we introduce the discrete maximum norm

$$\|v\|_{0,\infty,h} = \max_{\mathbf{x} \in E} |v(\mathbf{x})|, \quad E \subset \Omega_h.$$

In addition, we define the absolute error and relative error in the domain  $\Omega$  as follows:

$$\mathcal{E}_a^{in} = \|u(\mathbf{x}) - u_{dl}(\mathbf{x})\|_{0,\infty,h}, \quad \mathcal{E}_r^{in} = \left\| \frac{u(\mathbf{x}) - u_{dl}(\mathbf{x})}{u(\mathbf{x})} \right\|_{0,\infty,h}, \quad \mathbf{x} \in E = \Omega \cap \Omega_h.$$

The absolute error and relative error on the boundary  $\Gamma$  are defined by

$$\mathcal{E}_a^{bd} = \|u(\mathbf{x}) - u_{dl}(\mathbf{x})\|_{0,\infty,h}, \quad \mathcal{E}_r^{bd} = \left\| \frac{u(\mathbf{x}) - u_{dl}(\mathbf{x})}{u(\mathbf{x})} \right\|_{0,\infty,h}, \quad \mathbf{x} \in E = \Gamma \cap \Omega_h.$$

## 4.1 Elliptic PDEs

Consider the Poisson equation with the Dirichlet boundary

$$\begin{cases} -\Delta u = f & \text{in } \Omega, \\ u = g & \text{on } \Gamma, \end{cases}$$

where  $\Omega = (0,1)^d$  for  $d = 2$  and  $3$ . We choose appropriate  $f$  and  $g$  such that the exact solution yields

$$u(\mathbf{x}) = \sum_{i=1}^d (\sin(2\pi x_i) + 1.25).$$

In this experiment, we adopt  $h = 2^{-5}$  to generate the set  $\Omega_h$  as the test locations.

### 4.1.1 The 2D case

We first solve the above problem by the ALDL method with different parameters  $\beta$ . The test errors are presented in Figure 1 and in Table 1. It can be seen from Figure 1 (left) that the ALDL method is rather robust with respect to  $\beta$ , and there is no evident difference on the accuracy (within the domain) and convergent speed when  $\beta$  is chosen from 20 to 1000. In other words, one may use a relatively small  $\beta$  in practice. By Figure 1 (right), we can also see the ALDL method admits very good accuracy on the boundary.

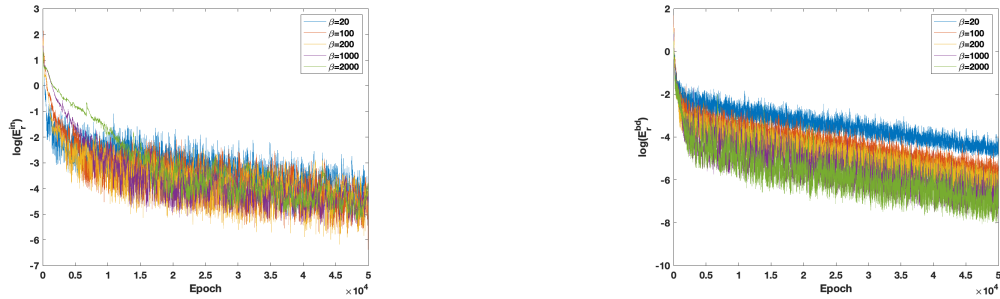


Figure 1: The relative error in the domain (left) and on the boundary (right) with ALDL.

$\beta$	$\mathcal{E}_r^{in}$	$\mathcal{E}_r^{bd}$
20	1.1117e-2	1.1291e-2
100	5.4996e-3	2.8480e-2
200	8.4536e-3	1.6015e-3
1000	1.3070e-2	1.5150e-3
2000	1.8460e-2	2.3461e-3

Table 1: The final relative errors of ALDL.

$\beta$	$\mathcal{E}_r^{in}$	$\mathcal{E}_r^{bd}$
200	8.0940e-2	2.5878e-2
1000	1.3468e-2	6.6136e-2
2000	1.0607e-2	4.0250e-3
10000	8.2640e-3	1.3014e-3
20000	4.9079e-2	1.0615e-3

Table 2: The final relative errors of PMDL.

We also solve the problem with the PMDL method with different parameters  $\beta$ , and the numerical results are shown in Figure 2 and Table 2. By Figure 2 (right) we can observe that one should use a large parameter  $\beta$  to get a good accuracy on the boundary. However, by Figure 2 (left) we can see that the large the parameter  $\beta$  is, the slower the converge rate. This may be due to the ill-conditioning for a relatively large  $\beta$  in the penalty methods [29].

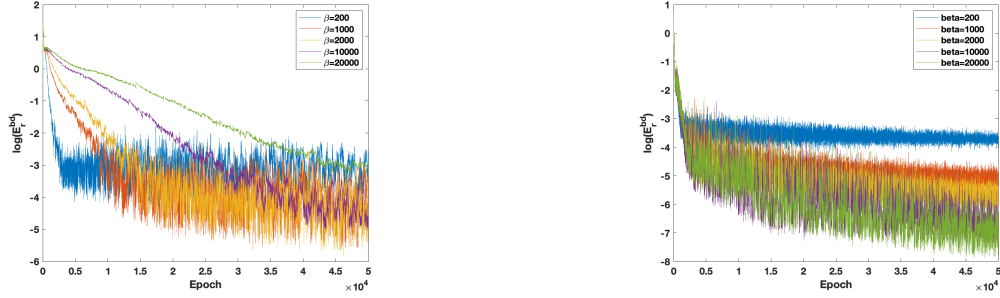


Figure 2: The relative error in the domain (left) and on the boundary (right) of PMDL.

To better present the numerical performance between the ALDL method and the PMDL method, we learn by Figure 1 and Figure 2 that the ALDL method behaves worst for  $\beta = 2000$  and best for  $\beta = 200$ , while the PMDL method behaves best for  $\beta = 2000$ . We then plot the results for both methods in Figure 3, and it is clear seen that the ALDL method still outperform the PMDL method.

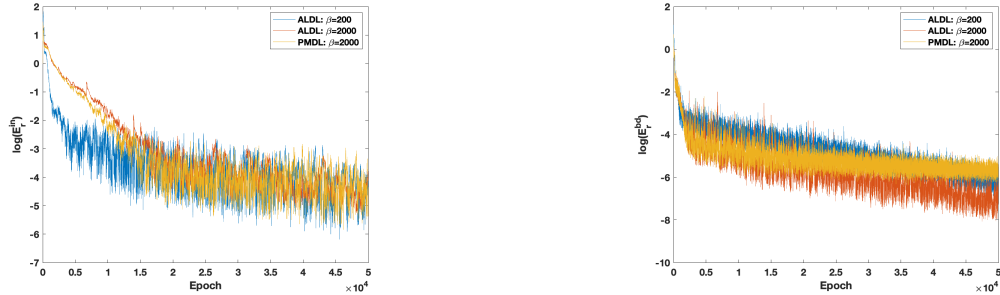


Figure 3: The relative error in the domain (left) and on the boundary (right).

#### 4.1.2 The 3D case

We next consider the three dimensional case. Similar plots are shown in Figure 4 and Figure 5, and the final approximation errors are listed in Table 3, Table 4. From those pictures and tables, one can draw similar conclusions as in the two dimensional case. We have also plotted the relative

errors of the two methods with different parameters in Figure 6. It is observed that both methods admit similar accuracy for relatively small  $\beta$ . However, in case of large parameters, the ALDL method outperforms the PMDL method.

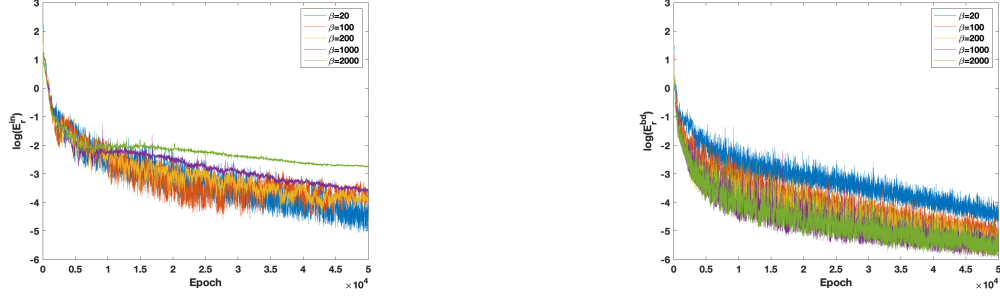


Figure 4: The relative error in the domain (left) and on the boundary (right) of ALDL.

$\beta$	$\mathcal{E}_r^{in}$	$\mathcal{E}_r^{bd}$
20	1.6577e-2	1.2226e-2
100	2.2614e-2	5.6861e-3
200	1.8200e-2	5.1053e-3
1000	2.7612e-2	4.2227e-3
2000	6.3994e-2	4.2941e-3

Table 3: The final relative errors of ALDL.

$\beta$	$\mathcal{E}_r^{in}$	$\mathcal{E}_r^{bd}$
200	2.8158e-2	2.4142e-2
1000	1.2118e-2	5.6179e-3
2000	2.9529e-2	4.7305e-3
10000	6.3245e-2	4.4151e-3
20000	9.0375e-2	6.6180e-3

Table 4: The final relative errors of PMDL.

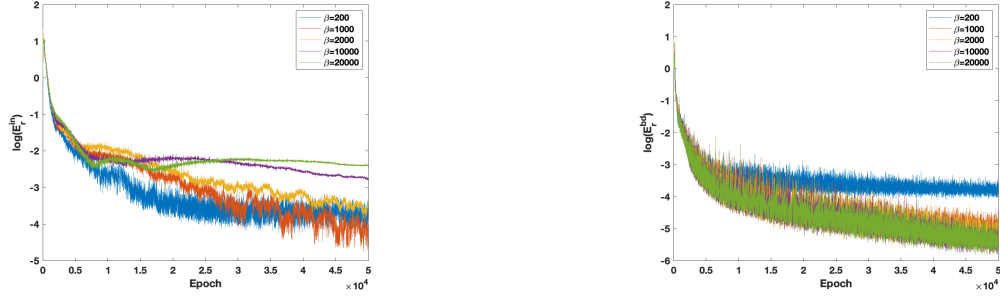


Figure 5: The relative error in the domain (left) and on the boundary (right) of PMDL.

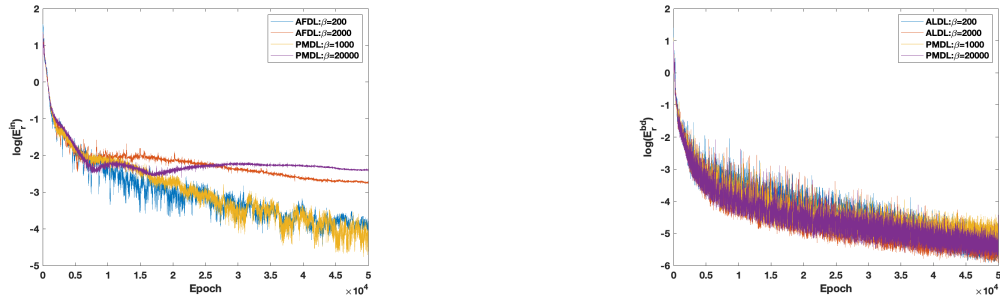


Figure 6: The relative error in the domain (left) and on the boundary (right) of different methods.

## 4.2 Linear eigenvalue problems

We next consider the following eigenvalue problem

$$\begin{cases} -\Delta u = \rho u & \text{in } \Omega, \\ u = 0 & \text{on } \Gamma, \end{cases}$$

where  $\Omega = (0, 1)^d$  for  $d = 2$  and  $3$ . The exact smallest eigenvalue is  $d\pi^2$  and the corresponding eigenfunction is

$$u(\mathbf{x}) = \prod_{i=1}^d \sin(\pi(x_i - 1)).$$

In this experiment, we adopt  $h = 2^{-4}$  to generate the set  $\Omega_h$  as the test locations. Due to the homogeneous Dirichlet boundary, we evaluate different approaches with absolute errors for eigenfunctions (and relative errors for eigenvalues).

### 4.2.1 The 2D case

We present the numerical results by the ALDL method with different parameters  $\beta$  in Figure 7 and Table 5. We can see that the numerical error is approximately  $10^{-3}$  for the eigenfunctions and  $10^{-4}$  for eigenvalues. Moreover, the approximation accuracy and convergence rate are robust with respect to different  $\beta$ .

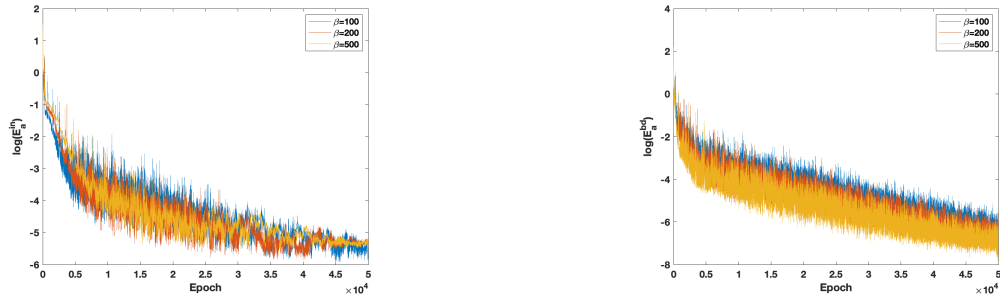


Figure 7: The absolute error in the domain (left) and on the boundary (right) of ALDL.

$\beta$	$\mathcal{E}_a^{in}$	$\mathcal{E}_a^{bd}$	$ \rho_{dl} - \rho /\rho$
100	3.6158e-3	1.5392e-3	4.6131e-4
200	5.4064e-3	1.8611e-3	4.6127e-4
500	4.9669e-3	1.3732e-3	1.5555e-4

Table 5: The final absolute errors of ALDL.

$\beta$	$\mathcal{E}_a^{in}$	$\mathcal{E}_a^{bd}$	$ \rho_{dl} - \rho /\rho$
1000	1.1452e-2	1.2916e-2	1.5981e-2
2000	8.0580e-3	7.8553e-3	8.8963e-3
20000	3.4719e-2	7.9888e-4	6.4343e-5

Table 6: The final absolute errors of PMDL.

We also show the associated results by the PMDL method in Figure 8 and Table 6, from which we may conclude that the accuracy and convergent speed of the PMDL method are relatively sensitive to the parameter  $\beta$ . The comparison between the ALDL method and the PMDL method are presented in Figure 9, and we can easily see that the ALDL method admits higher numerical accuracy and faster convergent speed than the PMDL method.

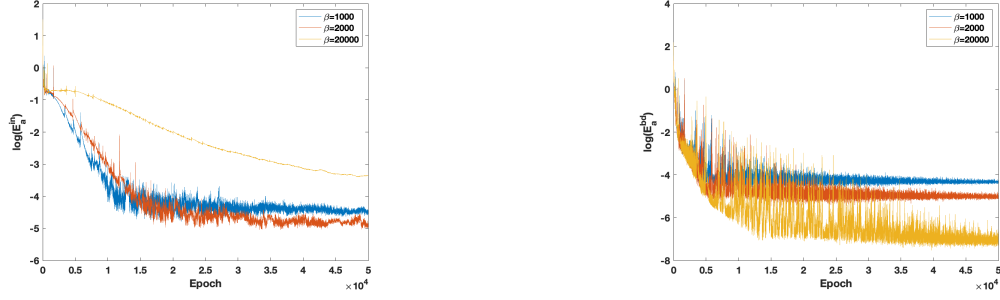


Figure 8: The absolute error in the domain (left) and on the boundary (right) of PMDL.

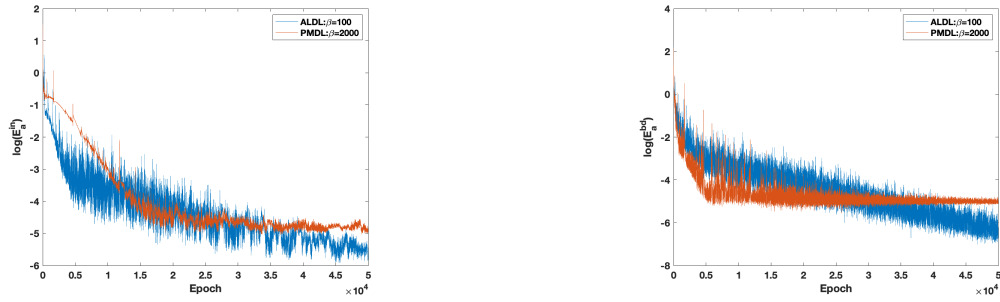


Figure 9: The absolute error in the domain (left) and on the boundary (right) of different methods.

#### 4.2.2 The 3D case

We have also performed the experiments for the three dimensional case, and the results are shown in Figure 10, Figure 11, and Table 7- Table 8. Similar to the two dimensional case, the ALDL method admits a better numerical performance in view of accuracy and convergent speed.

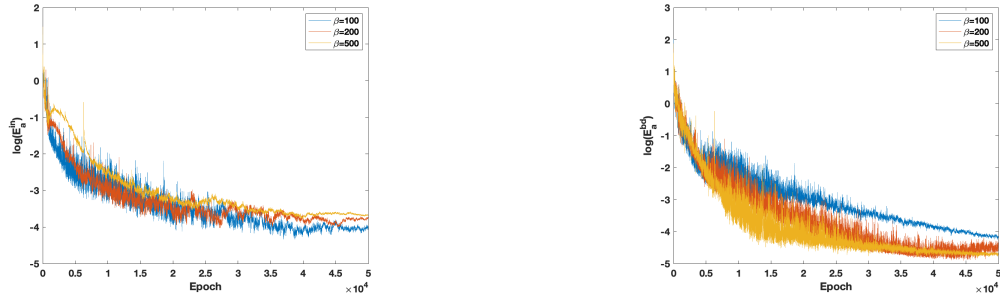


Figure 10: The absolute error in the domain (left) and on the boundary (right) of ALDL.

$\beta$	$\mathcal{E}_a^{in}$	$\mathcal{E}_a^{bd}$	$ \rho_{dl} - \rho /\rho$
100	1.7439e-2	1.5279e-2	1.2491e-4
200	2.4069e-2	1.1715e-2	4.1515e-4
500	2.5482e-2	8.9913e-3	3.5107e-4

Table 7: The final absolute error of ALDL.

$\beta$	$\mathcal{E}_a^{in}$	$\mathcal{E}_a^{bd}$	$ \rho_{dl} - \rho /\rho$
1000	2.8403e-2	1.9821e-2	1.4883e-2
2000	3.1909e-2	1.2343e-2	8.2697e-3
10000	9.1772e-2	1.0730e-2	2.1466e-4

Table 8: The final absolute error of PMDL.

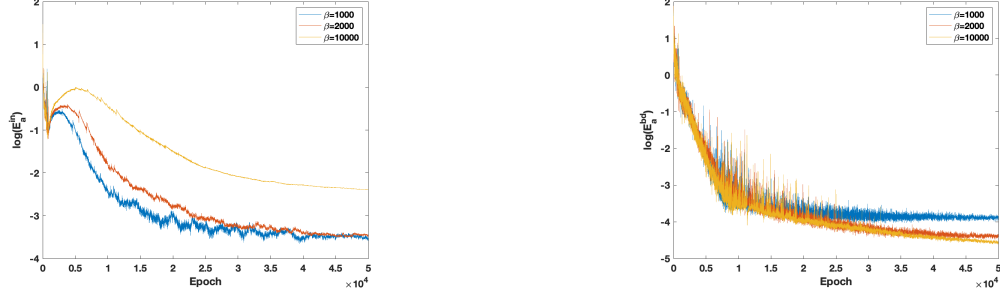


Figure 11: The absolute error in the domain (left) and on the boundary (right) of PMDL.

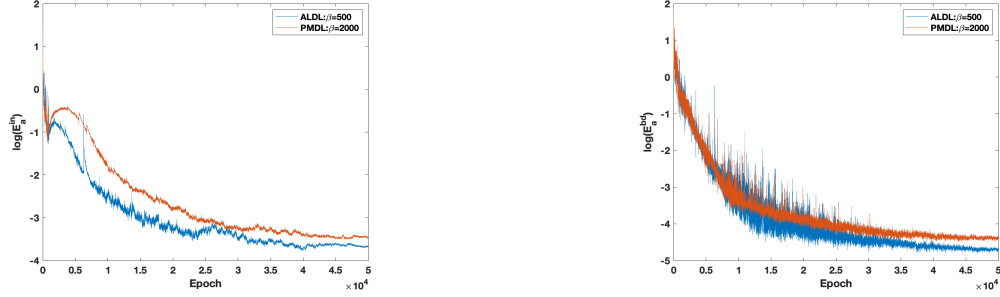


Figure 12: The absolute error in the domain (left) and on the boundary (right) of different methods.

### 4.3 A nonlinear eigenvalue problem

Finally, we consider the nonlinear Schrödinger eigenvalue problem

$$\begin{cases} -\Delta u + Vu + u^3 = \rho u & \text{in } \Omega, \\ u = 0 & \text{on } \Gamma, \\ \|u\|_{0,\Omega} = 1, \end{cases}$$

where  $\Omega = (0, 1)^d$  for  $d = 2$  and  $3$ , and  $V = \sum_{i=1}^d x_i^2$ . Since the true solutions  $\rho$  and  $u$  are unavailable, we shall numerical compute the reference solutions  $\rho_{ref}$  and  $u_{ref}$ . More precisely, we construct a DNN reference  $u_{ref}$  by:

$$u_{ref}(\mathbf{x}; \boldsymbol{\theta}) = \ell(\mathbf{x})\psi(\mathbf{x}; \boldsymbol{\theta}),$$

where  $\psi(\mathbf{x}; \boldsymbol{\theta})$  is a ResNet function with width 50 and depth 6, and

$$\ell(\mathbf{x}) = \prod_{i=1}^d x_i(1 - x_i).$$

In this way the reference solution admits a exact match on the boundary. The reference solution  $u_{ref}(\mathbf{x}; \boldsymbol{\theta})$  is trained by the Adam optimizer with a learning rate  $\eta = 5e - 4$ , and we set  $Epoch = 100000$  with batch size 2048 in the domain.

Similar to the linear eigenvalue problem, we adopt  $h = 2^{-4}$  to generate the set  $\Omega_h$  as the test locations.

#### 4.3.1 The 2D case

The numerical results for the ALDL method with different parameters  $\beta$  are presented in Figure 12 and Figure 13. Again, it is noticed that the method is insensitive to the choice of  $\beta$ .

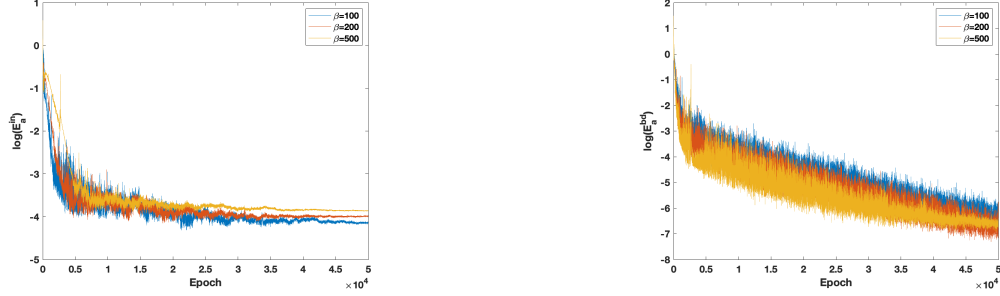


Figure 13: The absolute error in the domain (left) and on the boundary (right) of ALDL.

$\beta$	$\mathcal{E}_a^{in}$	$\mathcal{E}_a^{bd}$	$ \rho_{dl} - \rho_{ref} /\rho_{ref}$
100	1.5754e-2	2.7289e-3	7.4317e-3
200	1.8681e-2	1.2466e-3	6.7000e-3
500	2.1158e-2	1.3951e-3	6.3185e-3

Table 9: The final absolute errors of ALDL.

$\beta$	$\mathcal{E}_a^{in}$	$\mathcal{E}_a^{bd}$	$ \rho_{dl} - \rho_{ref} /\rho_{ref}$
1000	1.6011e-2	7.5234e-3	4.5439e-3
2000	1.8771e-2	3.7074e-3	3.1656e-4
20000	4.2896e-2	1.5495e-3	2.9424e-3

Table 10: The final absolute errors of PMDL.

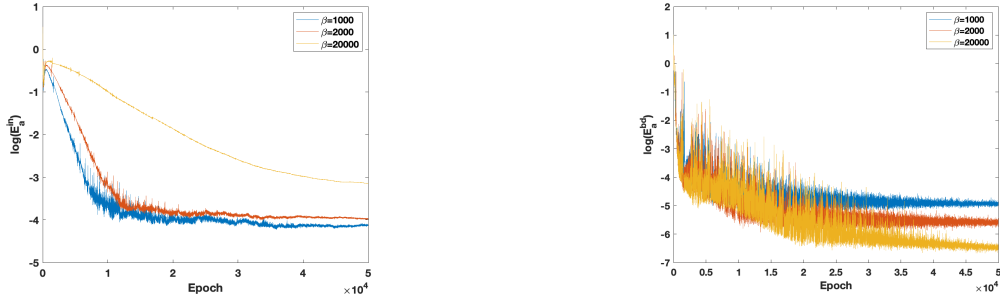


Figure 14: The absolute error in the domain (left) and on the boundary (right) of PMDL.

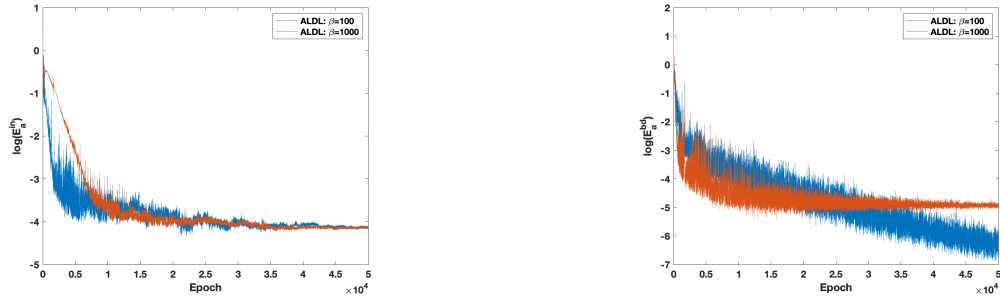


Figure 15: The absolute error in the domain (left) and on the boundary (right) of different methods.

The associated numerical results by the PMDL method are presented in Figure 14 and Table 10, from which we can see that the larger the  $\beta$  is, the slower the converge rate seems to be. The comparison between the ALDL method and the PMDL method are shown in Figure 15, from which we observe that the ALDL method admits a relatively faster convergent speed than the PMDL method.

### 4.3.2 The 3D case

We have also presented the 3D simulations, and the results are shown in Figure 16- Figure 18 and table 11 - 12, and one can draw similar conclusions as in the above examples.

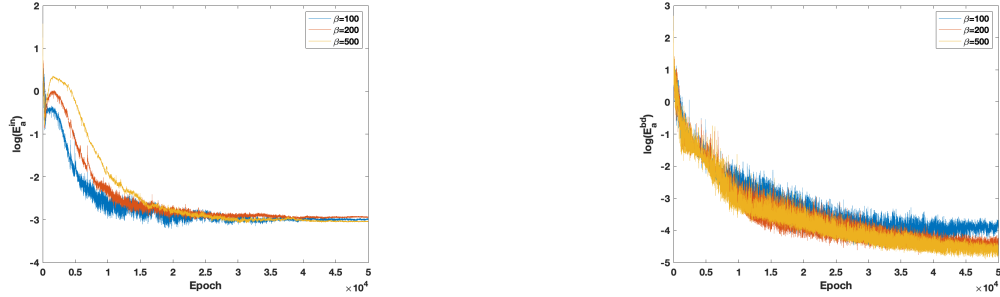


Figure 16: The absolute error in the domain (left) and on the boundary (right) of ALDL.

$\beta$	$\mathcal{E}_a^{in}$	$\mathcal{E}_a^{bd}$	$ \rho_{dl} - \rho_{ref} /\rho_{ref}$
100	5.0272e-2	2.2117e-2	6.2975e-4
200	5.2701e-2	1.1822e-2	1.2654e-3
500	4.7385e-2	1.0814e-2	6.2482e-4

Table 11: The final absolute error of ALDL.

$\beta$	$\mathcal{E}_a^{in}$	$\mathcal{E}_a^{bd}$	$ \rho_{dl} - \rho_{ref} /\rho_{ref}$
1000	4.4762e-2	2.4635e-2	8.4909e-3
2000	5.4154e-2	1.2571e-2	4.5849e-3
10000	2.9279e-1	1.3461e-2	4.7117e-3

Table 12: The final absolute error of PMDL.

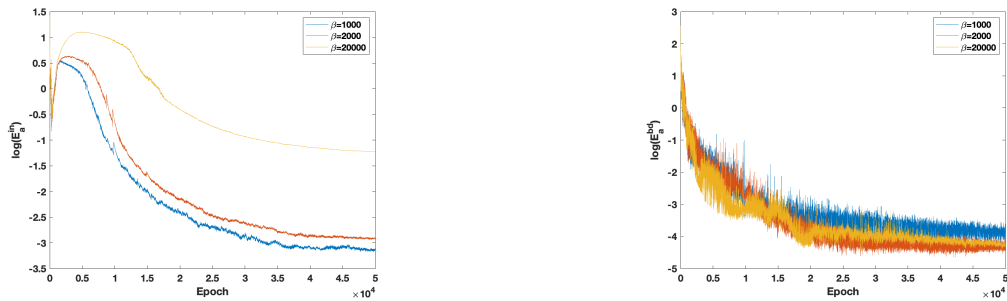


Figure 17: The absolute error in the domain (left) and on the boundary (right) of PMDL.

## 5 Concluding remarks

We have proposed an augmented Lagrangian deep learning method for variational problems with essential boundary conditions. The approach relies on first rewriting the original problems into an equivalent minimax problem, and then expressing the primal and dual variables with two individual



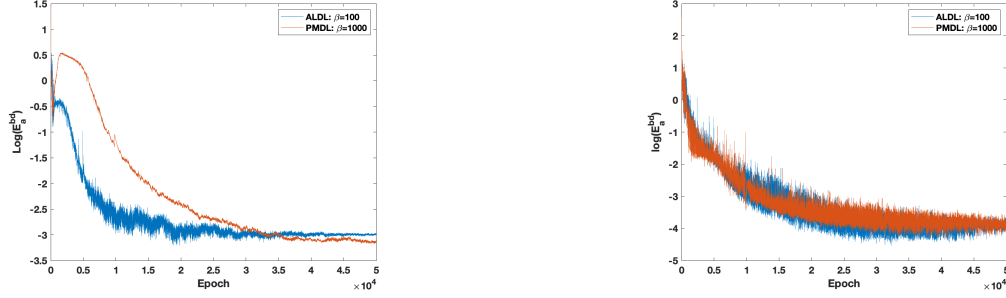


Figure 18: The absolute error in the domain (left) and on the boundary (right) of different methods.

DNN functions. Then, the network parameters of the primal and dual variables are trained using the stochastic optimization method together with a projection technique. Applications to elliptic problems and eigenvalue problems show that the ALDL method admits many advantages over the penalty method. In our future studies, we shall extend our ALDL approach to time dependent problems with complex solution structures.

## Acknowledgments

J. Huang was partially supported by NSFC (Grant No. 12071289) and Shanghai Municipal Science and Technology Major Project (2021SHZDZX0102). T.Zhou is supported by the National Key R&D Program of China (2020YFA0712000), NSFC (under grant numbers 11822111, 11688101), the science challenge project (No. TZ2018001), and youth innovation promotion association (CAS).

## References

- [1] R.A. Adams. *Sobolev Spaces*. Academic Press, New York, 1975.
- [2] A. Ambrosetti and A. Malchiodi. *Nonlinear Analysis and Semilinear Elliptic Problems*. Cambridge University Press, Cambridge, 2007.
- [3] A. R. Barron. Universal approximation bounds for superpositions of a sigmoidal function. *IEEE Transactions on Information Theory*, 39:930–945, 1993.
- [4] J. Berg and K. Nyström. A unified deep artificial neural network approach to partial differential equations in complex geometries. *Neurocomputing*, 317:28 – 41, 2018.
- [5] L. Bottou. Large-scale machine learning with stochastic gradient descent. In *Proceedings of COMP-STAT’2010*, pages 177–186, 2010.
- [6] S.C. Brenner and L. R. Scott. *The Mathematical Theory of Finite Element Methods (Third Edition)*. Springer, New York, 1994.
- [7] Cancès, E., R. Chakir, and Y. Maday. Numerical Analysis of Nonlinear Eigenvalue Problems. *J. Sci. Comput.*, 45:90–117, 2010.
- [8] Jean C  a. *Lectures on Optimization—Theory and Algorithms*. Tata Institute of Fundamental Research, Bombay, 1978.
- [9] F. Chen, J. Huang, C. Wang, and H. Yang. Friedrichs Learning: Weak Solutions of Partial Differential Equations via Deep Learning. *arXiv e-prints*, page arXiv:2012.08023, 2020.
- [10] P. G. Ciarlet. *Linear and Nonlinear Functional Analysis with Applications*. SIAM, Philadelphia, 2013.

- [11] P.G. Ciarlet. *The Finite Element Method for Elliptic Problems*. North-Holland, Amsterdam, 1978.
- [12] M. W. M. G. Dissanayake and N. Phan-Thien. Neural-network-based approximations for solving partial differential equations. *Comm. Numer. Methods Engrg.*, 10:195–201, 1994.
- [13] W. E. Machine learning and computational mathematics. *Commun. Comput. Phys.*, 28:1639–1670, 2020.
- [14] W. E, J. Han, and A. Jentzen. Deep learning-based numerical methods for high-dimensional parabolic partial differential equations and backward stochastic differential equations. *Commun. Math. Stat.*, 5:349–380, 2017.
- [15] W. E, C. Ma, and L. Wu. A priori estimates of the population risk for two-layer neural networks. *Commun. Math. Sci.*, 17:1407–1425, 2019.
- [16] W. E and B. Yu. The deep Ritz method: a deep learning-based numerical algorithm for solving variational problems. *Commun. Math. Stat.*, 6:1–12, 2018.
- [17] R. Glowinski and P. Le Tallec. *Augmented Lagrangian and Operator-splitting Methods in Nonlinear Mechanics*. SIAM, Philadelphia, 1989.
- [18] J. Han, A. Jentzen, and W. E. Solving high-dimensional partial differential equations using deep learning. *Proc. Natl. Acad. Sci. USA*, 115:8505–8510, 2018.
- [19] J. He, L. Li, J. Xu, and C. Zheng. ReLU deep neural networks and linear finite elements. *J. Comput. Math.*, 38:502–527, 2020.
- [20] K. He, X. Zhang, S. Ren, and J. FigSun. Deep residual learning for image recognition. In *2016 IEEE Conference on Computer Vision and Pattern Recognition (CVPR)*, pages 770–778, 2016.
- [21] K. Hornik, M. Stinchcombe, and H. White. Multilayer feedforward networks are universal approximators. *Neural Networks*, 2:359 – 366, 1989.
- [22] J. Huang, H. Wang, and H. Yang. Int-deep: A deep learning initialized iterative method for nonlinear problems. *J. Comput. Phys.*, 419:109675, 2020.
- [23] G.E. Karniadakis, I.G. Kevrekidis, L. Lu, P. Perdikaris, S. Wang, and L. Yang. Physics-informed machine learning. *Nat. Rev. Phys.*, 3:422–440, 2021.
- [24] D. P. Kingma and J. Ba. Adam: a Method for Stochastic Optimization. *arXiv e-prints*, page arXiv:1412.6980, 2014.
- [25] H. Lee and I. S. Kang. Neural algorithm for solving differential equations. *J. Comput. Phys.*, 91:110–131, 1990.
- [26] Y. Liao and P. Ming. Deep Nitsche method: Deep Ritz method with essential boundary conditions. *Commun. Comput. Phys.*, 29:1365–1384, 2021.
- [27] Z. Liu, W. Cai, and Z.-Q. J. Xu. Multi-scale deep neural network (MscaledNN) for solving Poisson-Boltzmann equation in complex domains. *Commun. Comput. Phys.*, 28:1970–2001, 2020.
- [28] J. Nitsche. Über ein Variationsprinzip zur Lösung von Dirichlet-Problemen bei Verwendung von Teilräumen, die keinen Randbedingungen unterworfen sind. *Abh. Math. Sem. Univ. Hamburg*, 36:9–15, 1971.
- [29] J. Nocedal and S. J. Wright. *Numerical Optimization*. Springer, New York, second edition, 2006.
- [30] M. Raissi, P. Perdikaris, and G.E. Karniadakis. Physics-informed neural networks: a deep learning framework for solving forward and inverse problems involving nonlinear partial differential equations. *J. Comput. Phys.*, 378:686 – 707, 2019.
- [31] Z. Shen, H. Yang, and S. Zhang. Deep network approximation characterized by number of neurons. *Commun. Comput. Phys.*, 28(5):1768–1811, 2020.

- [32] H. Sheng and C. Yang. PFNN: A penalty-free neural network method for solving a class of second-order boundary-value problems on complex geometries. *J. Comput. Phys.*, 428:110085, 2021.
- [33] J. Sirignano and K. Spiliopoulos. DGM: a deep learning algorithm for solving partial differential equations. *J. Comput. Phys.*, 375:1339 – 1364, 2018.
- [34] Rolf Stenberg. On some techniques for approximating boundary conditions in the finite element method. In *International Symposium on Mathematical Modelling and Computational Methods Modelling 94*, volume 63, pages 139–148. 1995.
- [35] Y. Zang, G. Bao, X. Ye, and H. Zhou. Weak adversarial networks for high-dimensional partial differential equations. *J. Comput. Phys.*, 411:109409, 14, 2020.
- [36] D. Zhang, L. Guo, and G. E. Karniadakis. Learning in modal space: solving time-dependent stochastic PDEs using physics-informed neural networks. *SIAM J. Sci. Comput.*, 42:A639–A665, 2020.